Improvement of Ethylene Removal Performance by Adsorption/Oxidation in a Pin-Type Corona Discharge Coupled with Pd/ZSM-5 Catalyst

Shirjana Saud [1], **Duc Ba Nguyen [1,2]**, **Seung-Geon Kim [1]**, **Ho Won Lee [1]**, **Seong Bong Kim [3]** **and Young Sun Mok [1,*]**

[1] Department of Chemical and Biological Engineering, Jeju National University, Jeju 63243, Korea; saudshirju@gmail.com (S.S.); band@plasma.ac.vn (D.B.N.); jyushin@jejunu.ac.kr (S.G.K.); hwlee@jejunu.ac.kr (H.W.L.)
[2] Center for Advanced Chemistry, Institute of Research and Development, Duy Tan University, 03 Quang Trung, Da Nang 550000, Vietnam
[3] Plasma Technology Research Center, National Fusion Research Institute, Jeollabuk-do 54004, Korea; sbkim@nfri.re.kr
[*] Correspondence: smokie@jejunu.ac.kr; Tel.: +82-64-754-3682; Fax: +82-64-755-3670

check for updates

Abstract: The adsorption and plasma-catalytic oxidation of dilute ethylene were performed in a pin-type corona discharge-coupled Pd/ZSM-5 catalyst. The catalyst has an adsorption capacity of 320.6 μmol g_{cat}^{-1}. The catalyst was found to have two different active sites activated at around 340 and 470 °C for ethylene oxidation. The removal of ethylene in the plasma catalyst was carried out by cyclic operation consisting of repetitive steps: (1) adsorption (60 min) followed by (2) plasma-catalytic oxidation (30 min). For the purpose of comparison, the removal of ethylene in the continuous plasma-catalytic oxidation mode was also examined. The ethylene adsorption performance of the catalyst was improved by the cyclic plasma-catalytic oxidation. With at least 80% of C_2H_4 in the feed being adsorbed, the cyclic plasma-catalytic oxidation was carried out for the total adsorption time of 8 h, whereas it occurred within 2 h of early adsorption in the case of catalyst alone. There was a slight decrease in catalyst adsorption capability with an increased number of adsorption cycles due to the incomplete release of CO_2 during the plasma-catalytic oxidation step. However, the decreased rate of adsorption capacity was negligible, which is less than one percent per cycle. Since the activation temperature of all active sites of Pd/ZSM-5 for ethylene oxidation is 470 °C, the specific input energy requirement by heating the feed gas in order to activate the catalyst is estimated to be 544 J/L. This value is higher than that of the continuous plasma-catalytic oxidation (450 J/L) for at least 86% ethylene conversion. Interestingly, the cyclic adsorption and plasma-catalytic oxidation of ethylene is not only a low-temperature oxidation process but also reduces energy consumption. Specifically, the input energy requirement was 225 J/L, which is half that of the continuous plasma-catalytic oxidation; however, the adsorption efficiency and conversion rate were maintained. To summarize, cyclic plasma treatment is an effective ethylene removal technique in terms of low-temperature oxidation and energy consumption.

Keywords: ethylene removal; Pd/ZSM-5; adsorption; corona discharge; plasma-catalytic oxidation

1. Introduction

Volatile organic compounds (VOCs) can be harmful to the environment and human health. Among many VOCs, ethylene is produced by agricultural commodities, which causes the ripening of fruits and vegetables [1–4]. Controlling the ethylene activity can lead to extending the postharvest shelf life

of fruits and vegetables [2]. Conventional techniques like ventilation, controlled atmosphere (CA), ozone treatment, oxidation, suppression of ethylene formation at plant receptor level can be used to control ethylene. Increased ventilation is associated with difficulty in controlling the parameters, like temperature and humidity, and CA is linked with a high cost/benefit ratio. Ozone treatment has been related to the reduction in the commercial value of fruits and vegetables due to injury [4].

Non-thermal plasma (NTP) has been widely used for the removal of VOCs [5–10], plant growth enhancement [11], particulate matter removal, and sterilization [12]. NTP induces highly chemical reactive species like electrons, ions, radicals, and ozone. Therefore, they can react with ethylene (C_2H_4) as well as VOCs under the close ambient temperature [4,6,7]. This is an advantage of NTP technology in the VOC removal process. A packed-bed dielectric barrier discharge (DBD) reactor has been widely used for the generation of plasma for the removal of VOCs and greenhouse gas [5,7,13,14]. However, in practical applications, the major issue with a packed-bed DBD reactor is high-pressure drop leading to high operation and maintenance costs. The reason is a tiny discharge gap at a few mm due to a high-voltage breakdown. Also, the amount of energy consumed for the generation of plasma is not feasible for practical applications. These challenges can be overcome with a corona discharge, which is well known for its lower power consumption (low current) and large discharge gap (avoid pressure drop). Hence, a corona discharge is a potential candidate for ethylene removal. Corona discharge can be generated by several configurations, namely, point to plane, wire to tubing/plane, and perforated disk to perforated disk [15–17]. Among them, the perforated disk to perforated disk configuration has promising practical applications and avoids pressure drop, due to the facilitated packed catalyst inside the discharge zone and the large discharge volume. Moreover, a large-scale plasma-catalyst for gas treatment would facilitate plasma discharge in a commercial honeycomb catalyst [15].

The relative humidity is also one of the major factors for ethylene production by fruits and vegetables at the storage and transportation level. Low relative humidity can be associated with water stress that causes weight loss of fruits and vegetables due to the drying out of surfaces [12]. Moreover, it also contributes to ethylene production. Therefore, the high performance of ethylene removal when carried out in a highly humid environment (relative humidity of 100%) is put forward, and is the condition used in this study. The ethylene concentration is usually low in agricultural storage in order of few parts per million (ppm) [2], meaning that continuous plasma generation for removal of such low concentrations of ethylene is unwanted. This work involves an investigation of the cyclic treatment process consisting of repetitive steps: (i) adsorption of ethylene on the catalyst and (ii) plasma catalytic oxidation to decompose adsorbed ethylene to recover the adsorption capability of the catalyst surface. Pd/ZSM-5 catalytic adsorbent prepared by ion exchange exhibits higher ethylene adsorbing capability even in 100% relative humidity (RH) [18].

This work focuses on the investigation of the adsorption/oxidation of dilute ethylene in the Pd/ZSM-5 catalyst coupled with corona discharge, perforated disk to perforated disk. Thermal programmed oxidation (TPO) of C_2H_4 over the catalyst was performed in order to determine the activation temperature of catalyst sites for the oxidation. The removal of C_2H_4 was examined under both continuous plasma-catalytic reaction and cyclic adsorption and plasma-catalytic oxidation. The evaluation of these processes was considered in terms of adsorption capacity, adsorption efficiency, the conversion rate of C_2H_4, and energy efficiency for C_2H_4 oxidation. A comparison among the thermal process, continuous plasma-catalytic reaction, and cyclic adsorption and plasma-catalytic oxidation was performed and discussed. The results showed that the cyclic adsorption and plasma-catalytic oxidation provides low-temperature oxidation of C_2H_4, improvement of adsorption performance, and energy efficiency for the removal of low-concentration of C_2H_4 (30 ppm) in the airflow.

2. Results and Discussion

2.1. Adsorption Capacity

The adsorption capacity of the catalyst is a critical factor in a cyclic adsorption-oxidation process, i.e., the long-term use of catalyst or the use of a catalyst with less weight and a decrease in the average power consumption for the oxidation step are results of a massive adsorption capacity. In this study, the adsorption capacity of Pd/ZSM-5 was examined under water vapor-saturated air containing 30 ppm C_2H_4 through 26-g Pd/ZSM-5 (packed in the pin-type corona reactor) at room temperature (~25 °C) for 240 h. The evolution of ethylene concentration under this condition is shown in Figure 1. As seen from this figure, the perfected adsorption of C_2H_4, more than 90% of ethylene in the gas inlet was absorbed by the catalyst, and this occurred within 1.2 h (initial time as shown in inset figure). Afterward, the concentration of C_2H_4 gradually increased and reached the inlet concentration (steady state of adsorption) at 14,136 min (~236 h). From the breakthrough curve, the adsorption capacity of Pd/ZSM-5 was estimated by an integration method (Equation (1)) to be 320.6 $\mu mol\ g_{cat.}^{-1}$. This capacity value has also been reported elsewhere [19]. To sum up, in the cyclic adsorption and plasma-catalytic oxidation of ethylene, adsorption time was designated to be 60 min.

$$\text{Adsorption Capacity} \left(\frac{\mu mol}{g} \right) = F * \frac{T * C_{in} - \int_0^T C_t dt}{W} \tag{1}$$

where F is the total flow rate in mol/min; T is the total adsorption time in min to obtain saturated adsorption; W represents the weight of catalyst used in gram; C_{in} and C_t denoted the concentration of ethylene in the gas inlet and gas outlet at time t, respectively, with unit of ppm.
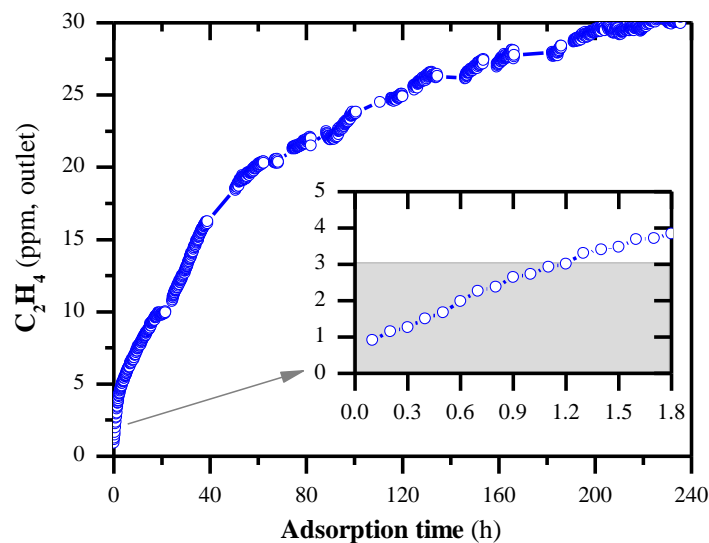
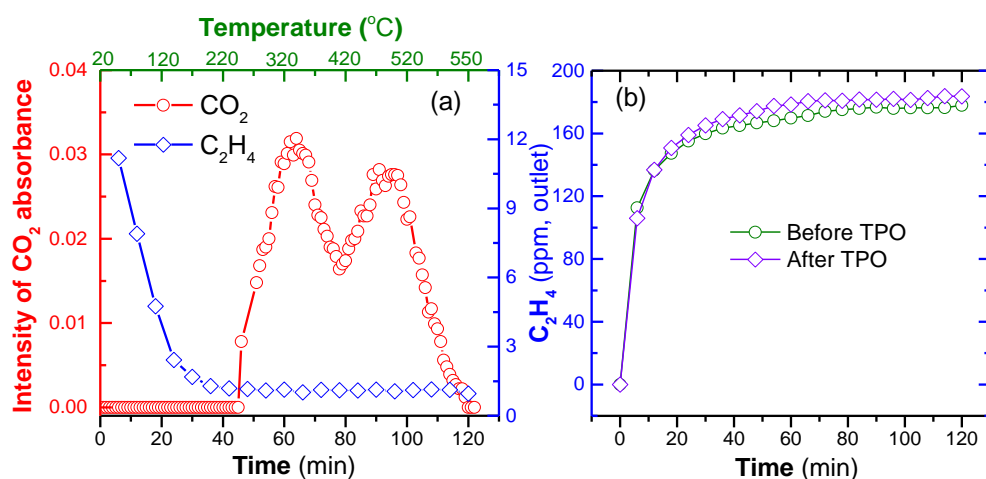**Figure 1.** Evolution of C_2H_4 concentration in the gas outlet of the corona discharge-coupled catalytic reactor (C_2H_4 concentration inlet: 30 ppm; Pd/ZSM-5: 26 g; total flow rate: 2 L/min).

2.2. Thermal-Programed Oxidization (TPO) of Ethylene

The TPO of C_2H_4 was performed without plasma, as shown in Figure 2a. C_2H_4 concentration of 200 ppm (2 L/min) was completely adsorbed on 5 g of the catalyst, which was packed into an alumina tube with an inner diameter of 15 mm, and then the temperature-programmed furnace was increased from 20 to 550 °C at a rate of 5 °C/min. Herein, before the adsorbed C_2H_4 performance, CO_2 and any impurities were desorbed from the Pd/ZSM-5 catalyst within 3 h at 300 °C by 2 L/min dry N_2. Here, the concentration of CO_2 was measured by a Fourier transform infrared spectrophotometer (Lambda Scientific, FTIR-7600, SA, Australia). The oxidation of adsorbed C_2H_4 started at 250 °C to form CO_2;

the peaks of CO_2 concentration were obtained at 340 °C and 470 °C. Subsequently, the concentration of CO_2 gradually approached zero. The results indicated the high reaction rate of C_2H_4 oxidation over the Pd/ZSM-5 catalyst from 340 °C. The appearance of two distinctive CO_2 peaks suggests that the Pd/ZSM-5 possesses two active sites, one being more highly active than the other. The earlier CO_2 peak at 340 °C indicates oxidation due to highly active sites. The later CO_2 peak at 470 °C illustrates the presence of an additional but less active site on the catalyst. The thermal programmed desorption of CO_2 over the Pd/ZSM-5 catalyst was also performed with the same conditions of the TPO process. CO_2 peak was not observed in the evolution of CO_2 intensity with the temperature range of 250 °C to 550 °C, suggesting that the two Pd/ZSM-5 active sites at 340 and 470 °C are C_2H_4 oxidation. As seen in Figure 2a, when heating up the system to the C_2H_4 oxidation initiation, there was a release of C_2H_4 in the gas outlet due to the desorption of C_2H_4. This suggests that the C_2H_4 oxidation step performed by a thermal process did not result in absolute oxidization of the adsorbed C_2H_4 over the catalyst to CO_2. A comparison of C_2H_4 adsorption between the fresh catalyst and spent catalyst (after TPO) was shown in Figure 2b. The adsorption was performed with the initial C_2H_4 concentration of 200 ppm and an adsorption time of 120 min. This figure clearly showed that the outlet concentration of the before TPO is lower than that of the after TPO at the same adsorption time. In other words, the adsorption capacity of the catalyst decreased after the TPO process, i.e., the adsorption capacity within 120 min adsorption time of the after TPO (66.5 μmol g_{cat}^{-1}) is 86.8% of the before TPO (76.7 μmol g_{cat}^{-1}). This result suggests that the adsorption capacity of the catalyst decreases toward the number of cycles of the thermal oxidation. Hence, in terms of practical applications, cyclic adsorption- thermal oxidation of C_2H_4 by the Pd/ZSM-5 has disadvantages including the C_2H_4 released during the early stage of oxidation and the decrease in adsorption capacity with the number of cycles, due to sintering behavior of Pd/ZSM-5 catalyst during the thermal process.


Figure 2. (**a**) TPO (temperature programmed oxidation) of C_2H_4 and (**b**) C_2H_4 adsorption of the catalyst before and after TPO (C_2H_4 concentration: 200 ppm; Pd/ZSM-5: 5 g; feed gas flow rate: 2 L/min).

2.3. Removal of C_2H_4 under the Continuous Operation of Plasma-Catalytic Reaction

Removal of C_2H_4 by the plasma-catalytic reaction was examined in the pin-type corona reactor under various input powers from 6 to 15 W with the total flow rate (100% RH) of 2 L/min consisting of 30 ppm C_2H_4, and O_2 as balance. Here, it should be noted that the 26 g of Pd/ZSM-5 catalyst was completely adsorbed by C_2H_4 before plasma turn-on, which avoided a decrease in the C_2H_4 concentration in the gas outlet due to the catalyst adsorption. Since the adsorption time was 236 h with a C_2H_4 concentration of 30 ppm in feed, the C_2H_4 concentration in feed was fixed at 2000 ppm instead of 30 ppm, allowing the adsorption time to be reduced, achieving a steady state within 11 h.

The C_2H_4 concentration in the outlet of the reactor was monitored under different supplied power, as shown in Figure 3a. As seen from the figure, the outlet C_2H_4 concentration initially varied with time and reached a steady state after the plasma-on time of 72 min. The instantaneous concentration of C_2H_4, as well as its concentration at steady-state, decreased with plasma-on time and input power. Generally, stronger plasma discharges are a result of an increase in input power; subsequently, more C_2H_4 in the feed can be decomposed under this condition. The conversion rate and energy efficiency at steady state were plotted in Figure 3b. The tendencies of conversion and energy efficiency are increasing with input power, except the energy efficiency at 15 W. This suggests the complete decomposition of C_2H_4 with a few remaining ppm of C_2H_4 that consume considerable input energy. This phenomenon is in line with the 20 ppm C_2H_4 decomposition in a fixed-bed dielectric barrier discharge reactor with the same catalyst, i.e., the energy requirement to 90% conversion of 20 ppm C_2H_4 in the feed was 80 J/L; however, in order to complete conversion of C_2H_4, its energy was 240 J/L [18]. To sum up, with 30 ppm C_2H_4 in the feed, the conversion rate obtained at 86% under the Pd/ZSM-5 catalyst conjugated with the corona discharge by a supplied power of 15 W (450 J/L).
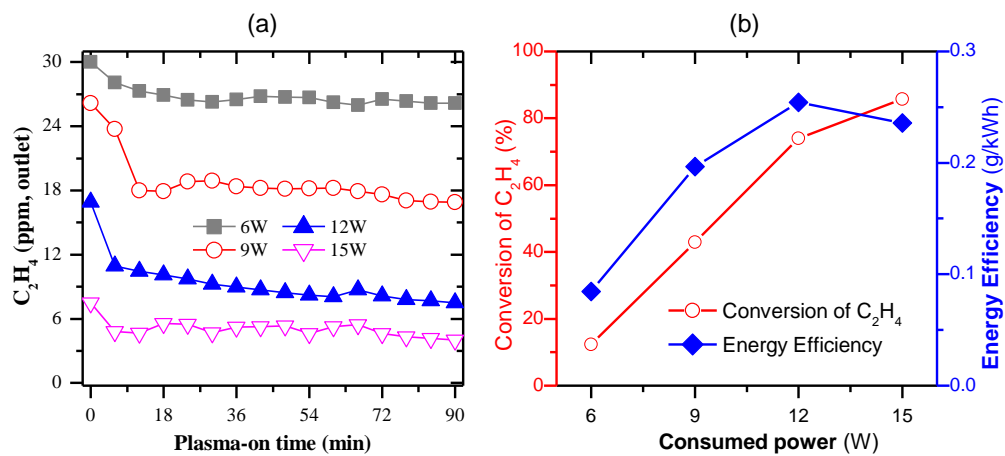
Figure 3. (**a**) Evolution of C_2H_4 continuous process of the plasma-catalytic process under different applied powers and (**b**) conversion rate and energy efficiency at steady state (total flow rate of 2 L/min included 30 ppm C_2H_4 and O_2 as balance).

For a target of practical applications in the storage unit or agricultural area, using oxygen plasma is not a feasible idea in comparison with air plasma (fed by ambient air). Thus, the effect of plasma gases (O_2/air) on the oxidation of C_2H_4 by the corona discharge was examined under the consumed power from 4 to 15 W. Figure 4 demonstrates that the conversion of C_2H_4 by air plasma was higher than that of O_2 plasma under the same consumed power. For instance, in order to achieve the conversion of 86% of 30 ppm C_2H_4 in feed, the consumed power of air was 9 W, while it was 15 W for the O_2 plasma case. Moreover, the conversion was 43% at a consumed power of 9 W in the O_2 plasma. As a result, the conversion of air plasma is twice times that of O_2 plasma at the consumed power of 9 W. Based on observing the plasma discharge during experiments, air discharge has a frequency transition from corona discharge to arc discharge in comparison to that of O_2 discharge at the same conditions. This phenomenon can be explained by the presence of more streamers of the plasma discharge with the presence of N_2 in the plasma gas. Nguyen and Lee [20] indicated the dielectric barrier discharge of N_2 as dilution gas has more streamers than other gas dilutions (He, Ar); this result supports the hypothesis. Consequently, air plasma provides high energy efficiency for C_2H_4 oxidation by the corona discharge; however, the frequent transition of the discharge to arcing needs to be solved. For further experiments in this study, oxygen is used as a plasma gas for the C_2H_4 plasma-catalytic oxidation step.
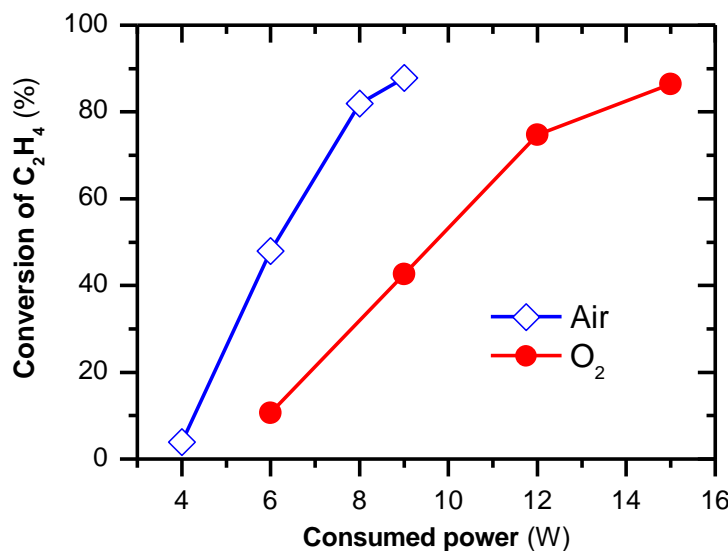
Figure 4. A comparison between air and oxygen as an oxidizing gas in the feed under various consumed power (total flow rate of 2 L/min included 30 ppm C_2H_4).

2.4. Removal of C_2H_4 by a Cyclic Adsorption-Plasma Oxidation Process

As seen in the above results, a combination of the corona discharge with the Pd/ZSM-5 is effective for the oxidation of C_2H_4. Also important is that the catalyst is capable of adsorption of more than 90% of 30 ppm C_2H_4 in the feed within 1.2 h. This suggests that cyclic adsorption and plasma-catalytic oxidation would reduce energy consumption and even obtain high-efficiency removal of C_2H_4. In this study, cyclic adsorption and plasma-catalytic oxidation for C_2H_4 removal were investigated under 60 min adsorption and 30 min plasma-catalytic oxidation per cycle with a total flow rate of 2 L/min and consisting of 30 ppm C_2H_4. According to the results from the continuous plasma discharge, more than 86% of C_2H_4 in the feed was oxidized under a consumed power of 15 W; consequently, its value was fixed during plasma-catalytic oxidation steps.

Figure 5a shows the concentration evolution of C_2H_4 and CO_2 during the adsorption and plasma-catalytic oxidation within 8 cycles. This figure demonstrates that there is a slight increase in the concentration of C_2H_4 in the gas outlet with the cycle number of the adsorption/oxidation. However, after 8 cycles, the C_2H_4 in the outlet was still less than 6 ppm and almost all of the potential adsorption of the catalyst was recovered by plasma-catalytic oxidation after each cycle. This also suggested that the adsorbed C_2H_4 had completely oxidized during the plasma-oxidation step. The CO_2 concentration during the oxidation step rapidly increased, reaching a maximum value and then gradually decreasing; however, the CO was not observed. The amount of C_2H_4 adsorption in each cycle was the area between the C_2H_4 concentration curve and the straight line at 30 ppm, which characterizes a constant input concentration; this area is superior to the area covered by the CO_2 concentration in each cycle. Moreover, the C_2H_4 molecules consist of two carbons. These phenomena suggest that CO_2 formation by the plasma-catalytic oxidation would be adsorbed by the catalyst and a slight decrease in the adsorption capacity of C_2H_4, which could be associated with the variation in the outlet CO_2 concentration during the oxidation step. Also, an increase in the amount of CO_2 emission from cycle to cycle can be linked with the release of the adsorbed CO_2. Indeed, the ratio of adsorption capacity between i cycle and first cycle and adsorption efficiency decreased with several cycles, as shown in Figure 5b. Specifically, from the first cycle to the 8th cycle, the ratio of adsorption capacity decreased from 100% to 95%, with an average decrease in adsorption capacity per cycle of 0.7%. This corresponds to the decrease in adsorption efficiency per cycle from 92% to 87%. To sum up, the plasma-catalytic oxidation by the corona discharge recovered the C_2H_4 adsorption capacity of the

Pd/ZSM-5. After 8 cycles, corresponding to a total adsorption time of 480 min, the adsorption capacity and adsorption efficiency were still 95% of the fresh catalyst and 87%, respectively.
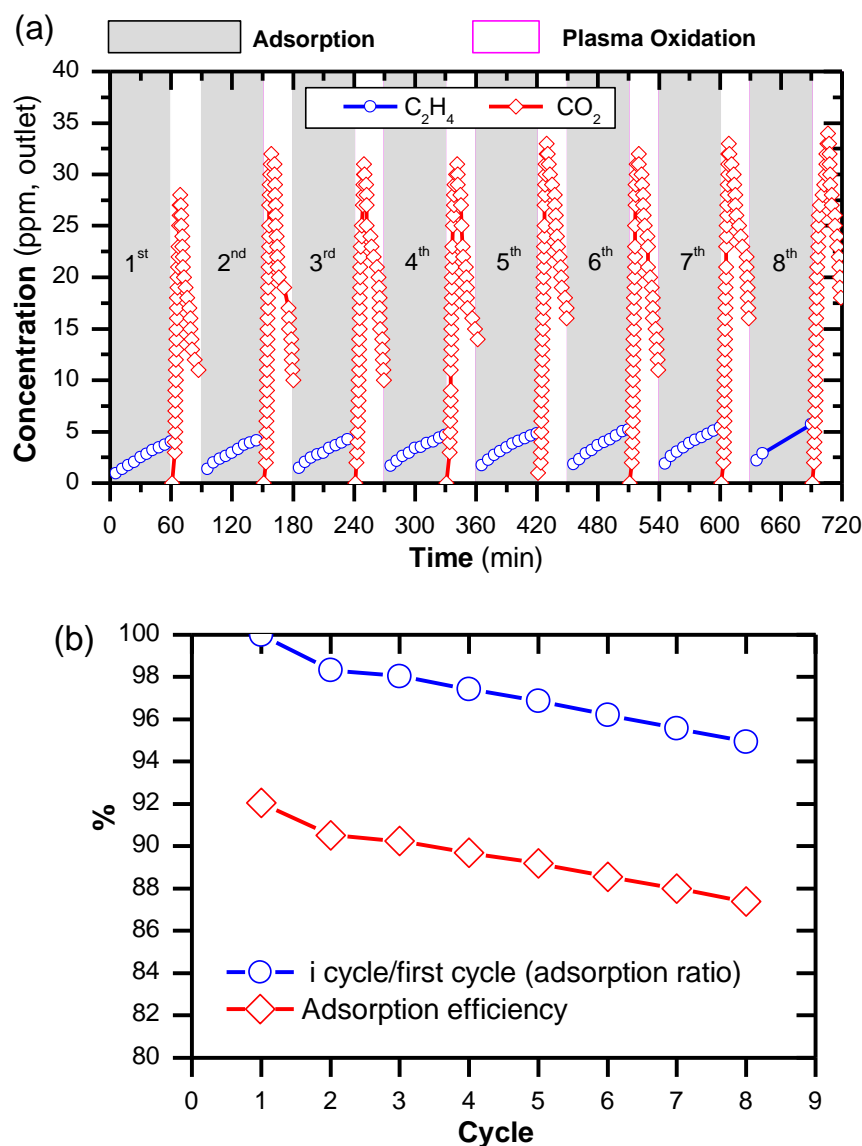
Figure 5. (**a**) Concentration of C_2H_4 and CO_2 in the gas outlet with adsorption and plasma-catalytic oxidation performed within 8 cycles, and (**b**) adsorption ratio between i cycle and first cycle, and adsorption efficiency as a function of a cycle number (in one cycle: adsorption time = 60 min and oxidation time = 30 min; total flow rate: 2 L/min: 30 ppm C_2H_4 in feed during adsorption steps during adsorption step, O_2 as feed gas and absence of C_2H_4 during the oxidation step, and the consumed power of 15 W).

To compare the adsorption performance of the continuous adsorption process with the intermittent adsorption process (the cyclic adsorption and plasma-catalytic oxidation), the concentration of C_2H_4 in the gas outlet was plotted in Figure 6. Herein, the adsorption time of each cycle was shifted total previous oxidation time; as a result, with 8 cycles the total adsorption time was 8 h. As seen from Figure 6, the adsorption performance improved with plasma-catalytic oxidation, i.e., the continuous process only kept the outlet concentration less than 6 ppm (80% of C_2H_4 in feed can be adsorption) within 2 h. Meanwhile, at all times in this experiment, the C_2H_4 in the gas outlet by intermittent adsorption was no larger than 6 ppm. From the breakthrough curve, the total amount of C_2H_4 adsorbed

on the Pd/ZSM-5 catalyst for 8 h was calculated to be 33.8 $\mu mol g_{cat}^{-1}$ for continuous adsorption and 41.1 $\mu mol g_{cat}^{-1}$ for cyclic treatment. This indicates that the adsorption capacity increased by 21.4% due to the incorporation of plasma-catalytic oxidation in the intermittent adsorption.
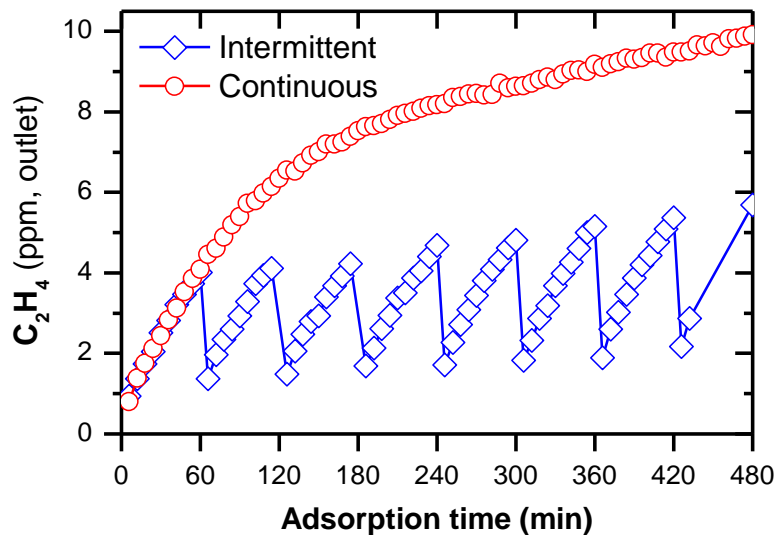
Figure 6. A comparison between continuous adsorption and intermittent adsorption (adsorption and plasma-catalytic oxidation).

To perform a comparison between thermal catalyst oxidation, plasma-catalytic oxidation, and cyclic adsorption and plasma-catalytic oxidation, the specific input energy (SIE) for these processes was calculated. According to TPO of C_2H_4, the operating temperature required to activate all catalyst sites is 470 °C, suggesting heating up the feed gas from 25 °C (room temperature) to 470 °C. The SIE for heating the feed gas can be estimated through Equation (2).

$$SIE \left(\frac{J}{kmol} \right) = \int_{T1}^{T2} C_P \, dT \tag{2}$$

Since the feed gas consisted of air and 30 ppm C_2H_4 and humidity, the specific input energy can be estimated through the heat capacity of air instead of the mixture of the feed gas. The heat capacity of air can be described as a function of temperature (T, K) by Equation (3) with the temperature from 50 to 1500 K [21].

$$C_P \left(\frac{J}{kmol \, K} \right) = C1 + C2 \left[\frac{\left(\frac{C3}{T} \right)}{\sinh \left(\frac{C3}{T} \right)} \right]^2 + C4 \left[\frac{\left(\frac{C5}{T} \right)}{\cosh \left(\frac{C5}{T} \right)} \right]^2 \tag{3}$$

Consequently, the integration of C_P from T1 to T2, SIE for heating air from T1 to T2 can be estimated by Equation (4).

$$SIE \left(\frac{J}{kmol} \right) = \left(C1 \, T + C2 \, C3 \coth \left(\frac{C3}{T} \right) - C4 \, C5 \tanh \left(\frac{C5}{T} \right) \right) \Big|_{T1}^{T2} \tag{4}$$

where: C1 = 28958, C2 = 9390, C3 = 3012, C4 = 7580, and C5 = 1484.

Using Equation (4), for heating the feed gas from room temperature (25 °C) to activation temperature of the Pd/ZSM-5 (470 °C), SIE was calculated to be 13,309,079 J/kmol, which corresponded

to 544 J/L. Meanwhile, the SIE of continuous plasma and adsorption and plasma-catalytic oxidation was calculated through Equations (5) and (6), respectively.

$$\text{SIE}\left(\frac{J}{L}\right) = \frac{60\, P(W)}{F\left(\frac{L}{min}\right)} \text{ for continuous plasma process} \tag{5}$$

$$\text{SIE}\left(\frac{J}{L}\right) = \frac{T_{oxidation}}{T_{adsorption}} \times \frac{60\, P\,(W)}{F\left(\frac{L}{min}\right)} \text{ for the adsorption and plasma-catalytic oxidation} \tag{6}$$

To sum up, the SIE for the thermal oxidation, continuous plasma oxidation, and the adsorption and plasma-catalytic oxidation are plotted in Figure 7. This figure indicates that the continuous plasma not only oxidizes the C_2H_4 at low temperature but also decreases the requirement of input energy (450 J/L) in comparison with the thermal oxidation process. Interestingly, the cyclic plasma process requires an average SIE of 225 J/L, which is half of the SIE in the continuous plasma. Here, it should be noted that the removal efficiency of C_2H_4 by the continuous plasma or cyclic plasma was similar; at least 86% of the 30 ppm C_2H_4 in the feed was oxidized through these processes. In terms of energy efficiency for C_2H_4 oxidation, the energy efficiency for the cyclic plasma was calculated to be 0.50 g/kWh, whereas the continuous plasma exhibited a lower energy efficiency of 0.23 g/kWh. Overall, the cyclic adsorption and plasma-catalytic oxidation improved in both of C_2H_4 removal performance and energy consumption.
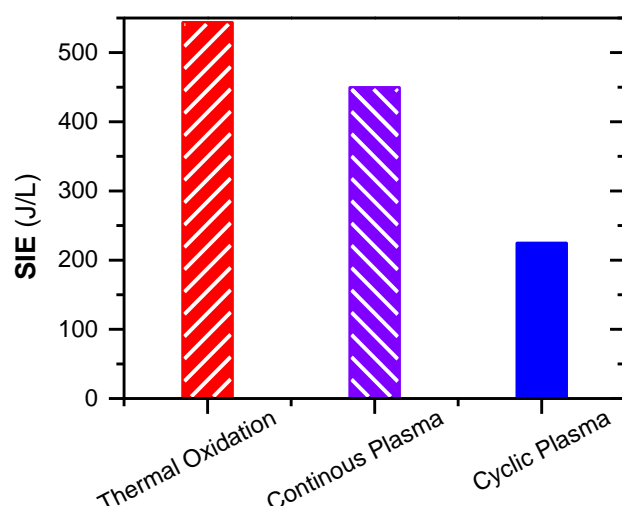

Figure 7. A comparison between continuous thermal/plasma catalyst oxidation with the cyclic adsorption and plasma-catalytic oxidation for the removal of 30 ppm C_2H_4 at a total flow rate of 2 L/min (adsorption time: 60 min; plasma-catalytic oxidation: 30 min; consumed power for plasma discharge: 15 W).

3. Materials and Methods

3.1. Synthesis of Pd/ZSM-5

The commercial pellet of zeolite ZSM-5 (average diameter: 3 mm, TOSOH Corporation) was chosen as a catalytic supporter for C_2H_4 removal. This Pd/ZSM-5 catalyst consisted of 0.36 wt.% Pd was prepared by the ion-exchange method, as shown elsewhere [18]. Briefly, 2 mM of precursor (PdCl$_2$) was mixed with 2 L of DI water and stirred for an hour for perfect mixing, as shown in Figure 8. The precursor solution was kept stirring at 25 °C, and was passed through 30 g of ZSM-5 zeolite for 24 h. The impregnated ZSM-5 was then washed off by passing DI-water through it for 2 h. The obtained

catalyst was dried at 110 °C for 12 h in a dry oven and subsequently calcined at 500 °C [22] for 3 h in an ambient air atmosphere using a muffle furnace.
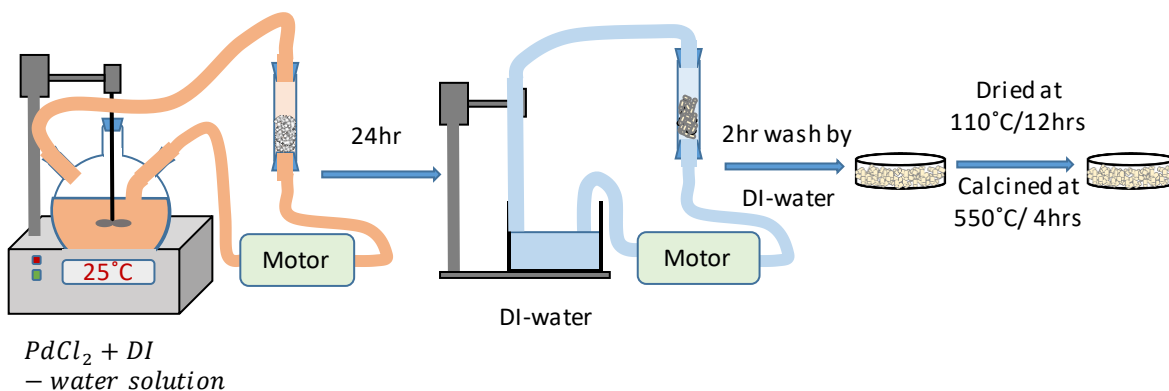
Figure 8. Catalyst preparation mechanism.

3.2. Experimental Setup

The adsorption and plasma-catalytic oxidation of dilute C_2H_4 were performed in a corona reactor coupled with the Pd/ZSM-5 catalyst, as shown in Figure 9. The pin-type corona reactor system is comprised of acrylic tubes, major tube (inner diameter: 115 mm, thickness: 3 mm) holding perforated ground electrode (diameter: 115 mm, thickness: 2 mm) and perforated high-voltage electrode (stainless steel; diameter: 85 mm, thickness: 2 mm) wrapped around Teflon (inner diameter: 62 mm) consisting 37 pins (diameter: 3 mm, length: 14.5 mm). 26 g of Pd/ZSM-5 covered one layer on the ground electrode surface. As a result, the distances from the pins to the surface of the catalyst and ground electrode were 27 and 30 mm, respectively. Consequently, the plasma discharge was a typical corona discharge in a conical shape of 134 mL. The C_2H_4 removal by the adoption and plasma-catalytic process included a 60 min adsorption step and then a 30 min plasma catalytic oxidation step in one cycle. All steps had the total flow rate fixed at 2 L/min and introduced to the reactor by mass flow controllers (MFCs). Here, the humidity of feed gas was carried out by a mixture of N_2 and O_2 (adsorption step) or O_2 (oxidation step) through a water bottle. For the adsorption step, the feed gas was a mixture of C_2H_4 (30 ppm, parts per million of volumetric) with the saturated air at ambient temperature; however, in the case of the oxidation step, it was O_2 and water vapor. Notably, the plasma was only turned on during the oxidation step; the plasma was driven by a direct current (DC) high voltage. For comparison, continuous plasma-catalytic treatment of C_2H_4 was also carried out with the same inlet concentration of C_2H_4 (30 ppm), but instead of the saturated air with the saturated O_2 in the feed.

During plasma discharge, the high voltage delivered on the power electrode was measured by a high-voltage probe (Tektronix P6015A) with an attenuation ratio of 1000:1; meanwhile, the digital signal was recorded by a digital oscilloscope (Tektronix DPO3034). The consumed power (P, watt) by the plasma process was monitored on the screen of the frequency converter regulator (KSP-1B). The C_2H_4 concentration in the gas outlet was analyzed by a gas chromatograph (Bruker 450-GC) equipped with a flame ionization detector (FID); while CO_2, a product by the plasma-catalytic reaction, was identified and quantified by a CO_2 monitor (ZG106R), and CO formation was monitored by a CO meter (TES 1372R) at the gas outlet. To analyze the definition of adsorption capacity and adsorption efficiency for a duration, conversion of C_2H_4 for continuous operation ($\eta_{continuous}$), as well as energy efficiency for C_2H_4 oxidation, is shown below:

$$\text{Adsorption Capacity for a cycle}\left(\frac{\mu mol}{g}\right) = F*\frac{(t2-t1)*C_{in} - \int_{t1}^{t2} C_t dt}{W} \qquad (7)$$

$$\text{Adsorption efficiency (\%)} = \left(1 - \frac{\int_{t1}^{t2} C_t dt}{(t2 - t1) * C_{in}} \right) * 100\% \tag{8}$$

$$\eta_{\text{continuous (\%)}} = \frac{C_{in} - C_o}{C_{in}} * 100\% \tag{9}$$

$$\text{Energy efficiency} \left(\frac{g}{kWh} \right) = \frac{\text{Weight of } C_2H_4 \text{ oxidation (g)}}{\text{Power consumption (kWh)}} \tag{10}$$

where F is the total flow rate in mol/min; W represents the weight of the catalyst used in gram; C_{in}, C_t, and C_o denoted the concentration of C_2H_4 with a unit of ppm in the gas inlet, gas outlet at time t, and gas outlet at the steady-state for continuous operation.
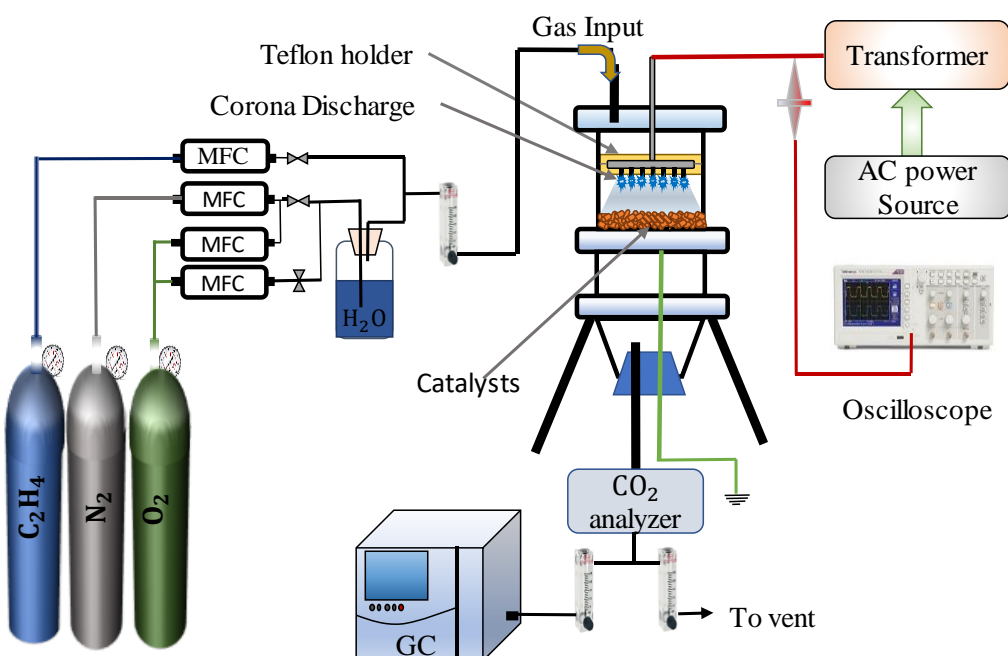
Figure 9. Schematic diagram of the Corona discharge-coupled catalytic reactor (CDCCR) system for removal of C_2H_4.

4. Conclusions

The Pd/ZSM-5 coupled with the pin-type corona discharge was used for the investigation of the removal of C_2H_4. The reactor was operated in cyclic mode: the adsorption step (60 min) and plasma-catalytic oxidation step (30 min). The catalyst featured high C_2H_4 adsorption capacity of 320.6 μmol g_{cat}^{-1}. The plasma-catalytic reaction at consumed power of 15 W showed effective removal of C_2H_4, at least 86% C_2H_4 in the feed oxidized to form CO_2. Consequently, the adsorption performance of C_2H_4 was improved with the cyclic adsorption and plasma-catalytic oxidation at a consumed power fixed at 15 W. The cyclic adsorption and plasma-catalytic oxidation exhibited not only low-temperature oxidation of C_2H_4 but also enhanced energy efficiency for C_2H_4 oxidation. Specifically, the requirement of SIE of the cyclic plasma treatment was only about half of that in the continuous plasma or thermal process with a similar conversion rate and adsorption efficiency of C_2H_4. The results show promising removal of C_2H_4 by a cyclic adsorption/oxidation in the corona discharge coupled with the Pd/ZSM-5 catalyst.

Author Contributions: S.S. and D.B.N. carried out the experimental work and analyzed the data; S.-G.K. synthesized catalyst, H.W.L., and S.B.K. participated in the interpretation of the results; Y.S.M. supervised all of the study. All authors have read and agreed to the published version of the manuscript.

Conflicts of Interest: The authors declare no conflicts of interest.

References

1. Gandhi, M.S.; Ananth, A.; Mok, Y.S.; Song, J.I.; Park, K.H. Time dependence of ethylene decomposition and byproducts formation in a continuous flow dielectric-packed plasma reactor. *Chemosphere* **2013**, *91*, 685–691. [CrossRef] [PubMed]

2. Keller, N.; Ducamp, M.N.; Robert, D.; Keller, V. Ethylene removal and fresh product storage: A challenge at the frontiers of chemistry. Toward an approach by photocatalytic oxidation. *Chem. Rev.* **2013**, *113*, 5029–5070. [CrossRef] [PubMed]

3. El Blidi, A.; Rigal, L.; Malmary, G.; Molinier, J.; Torres, L. Ethylene removal for long term conservation of fruits and vegetables. *Food Qual. Prefer.* **1993**, *4*, 119–126. [CrossRef]

4. Oka, A.; Motodate, T.; Takahashi, K.; Takaki, K.; Koide, S. Influence of oxygen concentration on ethylene removal using dielectric barrier discharge. *Jpn. J. Appl. Phys.* **2015**, *4*, 5882.

5. Trinh, Q.H.; Gandhi, M.S.; Mok, Y.S. Adsorption and plasma-catalytic oxidation of acetone over zeolite-supported silver catalyst. *Jpn. J. Appl. Phys.* **2014**, *54*, 01AG04. [CrossRef]

6. Trinh, Q.H.; Mok, Y.S. Effect of the adsorbent/catalyst preparation method and plasma reactor configuration on the removal of dilute ethylene from air stream. *Catal. Today* **2015**, *256*, 170–177. [CrossRef]

7. Trinh, Q.H.; Lee, S.B.; Mok, Y.S. Removal of ethylene from air stream by adsorption and plasma-catalytic oxidation using silver-based bimetallic catalysts supported on zeolite. *J. Hazard. Mater.* **2015**, *285*, 525–534. [CrossRef] [PubMed]

8. Feng, X.; Liu, H.; He, C.; Shen, Z.; Wang, T. Synergistic effects and mechanism of a non-thermal plasma catalysis system in volatile organic compound removal: A review. *Catal. Sci. Technol.* **2018**, *8*, 936–954. [CrossRef]

9. Cools, P.; De Geyter, N.; Morent, R. Plasma-Catalytic Removal of VOCs. In *Plasma Catalysis: Fundamentals and Applications*; Tu, X., Whitehead, J.C., Nozaki, T., Eds.; Springer: Cham, Switzerland, 2019; pp. 145–180. ISBN 978-3-030-05189-1.

10. Vandenbroucke, A.M.; Morent, R.; De Geyter, N.; Leys, C. Non-thermal plasmas for non-catalytic and catalytic VOC abatement. *J. Hazard. Mater.* **2011**, *195*, 30–54. [CrossRef] [PubMed]

11. Zhang, J.J.; Jo, J.O.; Huynh, D.L.; Mongre, R.K.; Ghosh, M.; Singh, A.K.; Lee, S.B.; Mok, Y.S.; Hyuk, P.; Jeong, D.K. Growth-inducing effects of argon plasma on soybean sprouts via the regulation of demethylation levels of energy metabolism-related genes. *Sci. Rep.* **2017**, *7*, 41917. [CrossRef] [PubMed]

12. Fylladitakis, E.D.; Theodoridis, M.P.; Moronis, A.X. Review on the history, research, and applications of electrohydrodynamics. *IEEE Trans. Plasma Sci.* **2014**, *42*, 358–375. [CrossRef]

13. Trinh, Q.H.; Kim, S.H.; Mok, Y.S. Removal of dilute nitrous oxide from gas streams using a cyclic zeolite adsorption-plasma decomposition process. *Chem. Eng. J.* **2016**, *302*, 12–22. [CrossRef]

14. Nguyen, D.B.; Nguyen, V.T.; Heo, I.J.; Mok, Y.S. Removal of NO_x by selective catalytic reduction coupled with plasma under temperature fluctuation condition. *J. Ind. Eng. Chem.* **2019**, *72*, 400–407. [CrossRef]

15. Mizuno, A.; Craven, M. Plasma Catalysis Systems. In *Plasma Catalysis: Fundamentals and Applications*; Tu, X., Whitehead, J.C., Nozaki, T., Eds.; Springer: Cham, Switzerland, 2019; pp. 21–46. ISBN 978-3-030-05189-1.

16. Tendero, C.; Tixier, C.; Tristant, P.; Desmaison, J.; Leprince, P. Atmospheric pressure plasmas: A review. *Spectrochim. Acta Part B At. Spectrosc.* **2006**, *61*, 2–30. [CrossRef]

17. Kim, K.N.; Lee, S.M.; Mishra, A.; Yeom, G.Y. Atmospheric pressure plasmas for surface modification of flexible and printed electronic devices: A review. *Thin Solid Films* **2016**, *598*, 315–334. [CrossRef]

18. Mok, Y.S.; Kim, S.G.; Ba Nguyen, D.; Trinh, Q.H.; Lee, H.W.; Kim, S.B. Plasma-catalytic oxidation of ethylene over zeolite-supported catalysts to improve the storage stability of agricultural products. *Catal. Today* **2019**, *337*, 208–215. [CrossRef]

19. Mok, Y.S.; Kim, S.G.; Nguyen, D.B.; Trinh, Q.H.; Lee, H.W.; Kim, S.B. Removal of dilute ethylene using repetitive cycles of adsorption and plasma-catalytic oxidation over Pd/ZSM-5 catalyst. *J. Phys. D Appl. Phys.* **2020**. Submitted Manuscript.

20. Nguyen, D.B.; Lee, W.G. Effects of ambient gas on cold atmospheric plasma discharge in the decomposition of trifluoromethane. *RSC Adv.* **2016**, *6*, 26505–26513. [CrossRef]

21. Poling, B.E.; Thomson, G.H.; Friend, D.G.; Rowley, R.L.; Wilding, W.V. Section 2: Physical and Chemical Data. In *Perry's Chemical Engineers' Handbook*; The McGraw-Hill Companies, Inc.: New York, NY, USA, 2007; ISBN 0071542094.

22. Kucharczyk, B.; Szczygieł, B.; Chęcmanowski, J. The effect of catalyst precursors and conditions of preparing Pt and Pd-Pt catalysts on their activity in the oxidation of hexane. *Open Chem.* **2017**, *15*, 182–188. [CrossRef]